Conference Paper, Published Version

Ismail, Zulhilmi; Shiono, Koji

Computational of Flow Behaviours in Compound Meandering Channel with Non-Vegetated and Cross-Over Vegetated Floodplains

COMPUTATIONAL OF FLOW BEHAVIOURS IN COMPOUND MEANDERING CHANNEL WITH NON-VEGETATED AND CROSS-OVER VEGETATED FLOODPLAINS FOR OVERBANK FLOW

Zulhilmi Ismail[(1)], Koji Shiono[(2)]

[(1)]Researcher, Department of Hydraulics and Hydrology, Faculty of Civil Engineering, Universiti Teknologi Malaysia, 81310 Skudai Malaysia; e-mail: zulhilmi@utm.my
[(2)]Professor, Department of Civil and Building Engineering, Loughborough University, Loughborough, Leicestershire, LE11 3TU, UK; e-mail: k.shiono@lboro.ac.uk

ABSTRACT

Computational results concerning flow structures have been carried out in a meandering channel with simulated non-vegetated and vegetated floodplains for overbank flow. The effect of placing solid blocks as a model of rigid, unsubmerged floodplain vegetation on a floodplain adjacent to a meandering channel is considered. The aim was to investigate how the cross-over vegetated floodplain influence flow behaviours. Telemac 2D and 3D were applied to predict mean velocity and secondary flow. Detailed analyses of the predicted flow variables were therefore carried out in order to understand mean flow mechanisms and secondary flow structures in compound meandering channels. For the non-vegetated floodplain shows how the shearing of the main channel flow as the floodplain flow plunges into and over the main channel influences the mean and turbulent flow structures, particularly in the cross-over region. While applying vegetated floodplain along a cross-over section confirmed that the minimum/reduction shearing of the main channel flow by the floodplain flow plunging into and over the main channel is observed from the cross-sectional distributions of the streamwise velocity, lateral velocity, and secondary flow vectors.

Keywords: compound meandering channel, mean velocity, flow mechanisms and secondary flow.

1. INTRODUCTION

During the past decades, the conventional "flood control" ideology has evolved into a philosophy of "flood management". An effective flood management program must consider environmental, recreational, and aesthetic issues in addition to flood control. Riparian vegetation has become an integral component of the flood channel. Vegetation stabilises stream banks, provides shade that prevents excessive water temperature fluctuations, supports wildlife and performs a essential role in nutrient cycling and water quality. In addition, vegetation is an important feature of many rivers, providing habitat for other organisms and enhancing amenity values for people. Emergent vegetation occurs commonly along the banks of river and artificial channels, both naturally and by design for erosion and habitat creation. The effect of such marginal vegetation on flow resistance has been investigated for straight channels but a little known of its effects for meandering channels under either inbank or overbank flow conditions (Ishigaki et al, 2002).

The extensive research on flow resistance in compound straight and meandering channels with fixed and mobile beds and, rough and smooth floodplains have been carried out in Flood Channel Facility (FCF), HR Wallingford. Shiono and Muto (1998) studied the three-dimensional flow structures in meandering channels with overbank flow in detail, based on velocity measurement. They identified that the development of secondary flow for overbank flow structure is controlled by flow interaction in the cross-over section. They also found that the generation mechanisms of secondary flow and turbulence are totally different from those for the straight compound channel and that most mean energy loss occurs along the cross-over region (Shiono et al, 2001). To date, the effect of vegetation placing along the floodplain edges in compound meandering channel on flow has not been investigated yet. This paper uses computational modelling to address one of the objectives towards establishing a clear and improved understanding of the secondary flow structures in compound meandering channels. Telemac (Hervouet, 2000) is the suite of computer codes dedicated to the numerical simulation of free-surface flows developed by the Laboratoire National d'Hydraulique, Electricite de France (EDF). In the United Kingdom, the Telemac codes are distributed by Hydraulic Research (HR) Wallingford, UK. This paper focuses to show the effect of vegetation on flow behavior and mechanism in case of non-vegetation and vegetation placing along the cross-over section.

2. COMPUTATIONAL MODELLING

The development of computational models applicable to flows in compound meandering channels is still in its infancy. The problems that modellers encounter include grid calculation and the estimation of various factors which are supposed to be effective in determining flow behaviour. With respect to the grid system, curvilinear systems or element schemes can meet the requirement for irregular geometries. The behaviour, extent and strength of momentum exchange between the fast and slow fluids in the shallow shear layer are important in the compound channel flows. The momentum exchange; bed generated turbulence; secondary flow circulations and sudden expansion and contraction of the floodplain flows are some of the peculiar characteristics of the compound straight and meandering channels. The three-dimensional (3D) Reynolds-Averaged Navier-Stokes (*RANS*) and continuity equations describe turbulent free-surface flows that have a practical interest being commonly encountered in water and environmental engineering problems. Solving the full set of three-dimensional equations requires considerable time and computing resources.

Rameshwaran and Shiono (2002) used Telemac2D to predict the depth-averaged velocity and bed shear stress in a compound meandering channel with a natural cross-section. They reported calibrating the Manning's coefficient to achieve a uniform flow condition that was 18 % higher than the skin friction of the bed material. The velocity and bed shear stress were predicted reasonably well in the main channel using both the constant eddy viscosity and $k-\varepsilon$ turbulence model. A recent research trend shows the increasing use of commercially available, general-purpose, computational fluid dynamics (CFD) codes to study compound channels including Rameshwaran and Naden (2003). Three-dimensional computational fluid dynamics (CFD) models have since been increasingly used to predict compound channel flows and to assess the suitability of a range of turbulence models for simulating flow structures, particularly those generated by the main channel-floodplain interactions.

3. MESH GENERATION

The adaptive mesh generator called MATISSE provided within the framework of Telemac3D was used to generate the finite element unstructured triangular mesh. Telemac uses a two-dimensional (2D) mesh as a base mesh to construct the full three-dimensional (3D) mesh. The 2D mesh is an unstructured triangular mesh based on Delaunay Triangulation. The details of the 2D and 3D meshes and the number of horizontal levels used for the different flow cases are summarised in **Table 1. Fig. 1** shows the elevation view of the 3D mesh in the main channel at the bend apex for two different flow cases in Telemac 3D while **Figs. 2** and **3** show the plan view of the 2D base mesh (half-meander only) for both cases.

Table 1: Main summary of meshes for different simulation cases

Case	2D mesh (Triangular element)		3D mesh (Prismatic element)		No. of Horizontal planes
	Total nodes	Total elements	Total nodes	Total elements	
Non-Vegetated	22612	44573	63756	113520	12
Cross-over Vegetated	8070	15576	64788	114741	12

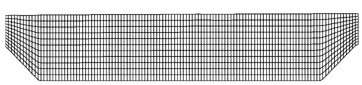

Figure 1

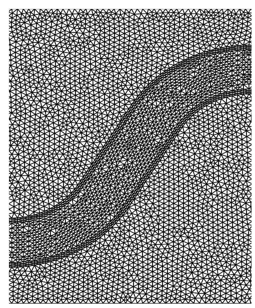

Figure 2

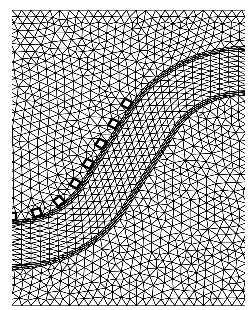

Figure 3

3.1 Initial and Boundary Conditions

In Telemac 2D the only way to achieve uniform flow without changing the experimental flow conditions is by changing either the Manning coefficient or the eddy viscosity. According to Spooner and Shiono (2003), the eddy viscosity does not significantly affect depth-averaged velocity distribution, therefore the Manning coefficient was adjusted. With the different arrangement of floodplain roughness and using the constant eddy viscosity, the calibrated Manning coefficients for uniform flow were obtained and are list in **Table 2**. The Plan of sign convention system for variable velocities and location details of the measurement of non-vegetated and cross-over vegetated floodplain are shown in **Figures 4** and **5** respectively.

Table 2: Manning coefficient, n for different simulation cases in Telemac 2D

Case	Manning's n	
	Dr = 0.25	Dr = 0.45
Non-Vegetated	0.01125	0.01175
Cross-over Vegetated	0.01100	0.01120

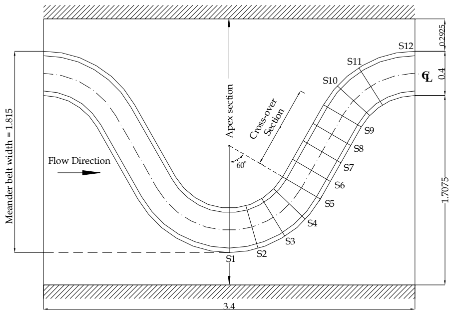

Figure 4

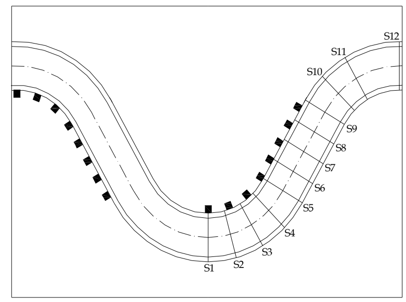

Figure 5

4. RESULTS AND DISCUSSIONS

4.1 Depth-averaged Velocity Vector Fields

Figures 6 and **7** show the results for the distribution of depth-averaged velocities along one meander wavelength for non-vegetated and cross-over vegetated floodplains respectively. Non-vegetated floodplain shows that the main channel flow deviates at an angle away from the meander streamline direction due to the strong floodplain flow, which predominantly follows the direction of the valley. This feature will cause the retardation of the flow within the meander belt, being slower than the outer side. On the other hand, from the middle part of the cross-over section, the velocity distribution becomes more uniform and its primary direction is streamwise. This is due to the flow structure in the main channel being significantly changed from the exit of the bend to the cross-over region. At the bend apex, it is also clear that the flow along the inner bank is faster than along the outer bank.

Figure 7 shows the results of vectors of depth-averaged velocities along one meander wavelength for cross-over vegetated floodplain. Figure shows that the overbank flows give the maximum velocity filament in the main channel occurs relatively near the outer bank sidewall at the upstream apex bed and continues to move steadily to the outer bank as it approaches the downstream bend apex. However, along the cross-over section many vortices occur near the inner bank of the main channel behind the blocks. However, the main channel flow predominantly follows the main channel direction at the outer bank of the main channel. At the end of the blocks in the cross-over section, interestingly, there are large vortices. These are produced by the interaction of the blocks and the floodplain flow because of the faster velocity from the floodplain being naturally concentrated due to the blocks at the end of the cross-over.

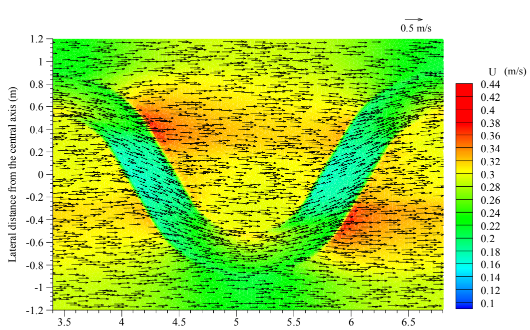

Figure 6: Depth-averaged velocity for non-vegetated floodplain

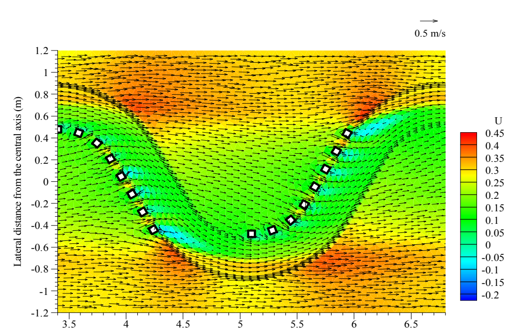

Figure 7: Depth-averaged velocity for cross-over vegetated floodplain

4.2. Three Dimensional Variable Velocities - Streamwise Velocity

Figures 8 and **9** show contour lines of streamwise velocities normalised by the sectional averaged velocity for non-vegetated and cross-over vegetated floodplain respectively at sections S1 to S12. **Figure 8** shows the cross-sectional distributions of the predicted streamwise velocity (U) for non-vegetated. Maximum streamwise velocity was observed to be $1.15U_s$ near the inner side of the main channel. Minimum streamwise velocity was found to be $0.55U_s$ near the bottom closer to the outer side of main channel.

In cross-over vegetated floodplain**, Figure 9** shows the distribution profile and the behaviour of the streamwise velocity are higher. Particularly at the bend section, the average maximum streamwise velocity is $1.2U_s$ above the bankful level of the main channel. In the cross-over region, most of the maximum streamwise velocity is seen at the outer (right) side. At the cross-over sections S5 to S7, the velocity at $y/h = 0$, (left hand side) is almost zero, which is totally different from those in non-vegetated floodplain, thus substantial reductions in shearing due to the floodplain flow plunging onto the main channel. Therefore the shear interaction between the floodplain flow and the main channel flow is significantly less taken place. However, there are distinct velocity difference between the upper layer and lower layer in the inner side of the main channel (i.e. slower flow in the upper layer and faster flow in the lower layer) even the large relative depth. This means that the flow in the lower layer is retardant, rather than acceleration by the upper layer flow in cases non-vegetated. At the cross-over section (sections S6 to S9), the minimum shearing of the main channel flow by the floodplain flow plunging into and over the main channel can be seen due to blocking the floodplain flow entering the main channel by the blocks.

4.3 Three Dimensional Variable Velocities - Lateral Velocity

Figure 10 shows at sections S1 and S2, the magnitudes of the lateral velocity are very small and the averages of around $0.1U_s$ and $0.2U_s$ respectively. The small magnitudes of lateral velocities are also seen at sections S3 and S4. As discussed earlier, at the apex section, since the main channel and floodplain flows are parallel to each other, the influence of the interaction between the two flows is less significant at the bend apex. However, from section S5 to section S9 the magnitude above the bankful level at the inner side of the main channel increases. The maximum lateral velocity is $0.7U_s$ at the inner bankful level of the main channel from section S4 to section S9, along the cross-over section, which is larger than the streamwise velocity; its influence area corresponds to the front. As the flow moves downstream to section S11, the magnitude above the bankful level starts to decrease to become weak at the front. Thus the figure clearly shows that the floodplain flow particularly becomes a strong influence in the cross-over region. As will be discussed in a later section, the secondary flow circulations in compound meandering channels are mainly generated due to the floodplain flow plunging the main channel flow at the bankful level in the cross-over region.

The lateral velocity shown in **Figure 11** has a quite complicated pattern of flow but there is a noticeable pattern of higher lateral velocities at the inner side of the main channel and relatively slower velocities near the bed of the bend apex section S1. Maximum positive lateral velocity is observed to be $0.3U_s$ and the minimum negative lateral velocity is observed to be $-0.1U_s$. The positive velocities increase gradually at the inner side of the main channel around $0.35U_s$, $0.5U_s$ and $0.6U_s$ at sections S2, S3 and S4 respectively. However, at the beginning of cross-over section, S5, a higher velocity starts to occur at the outer side above the bankful level of the main channel up to section S6 showing that the main channel flow escaping onto the floodplain. The complicated flows can be seen in sections S7, S8 and S9

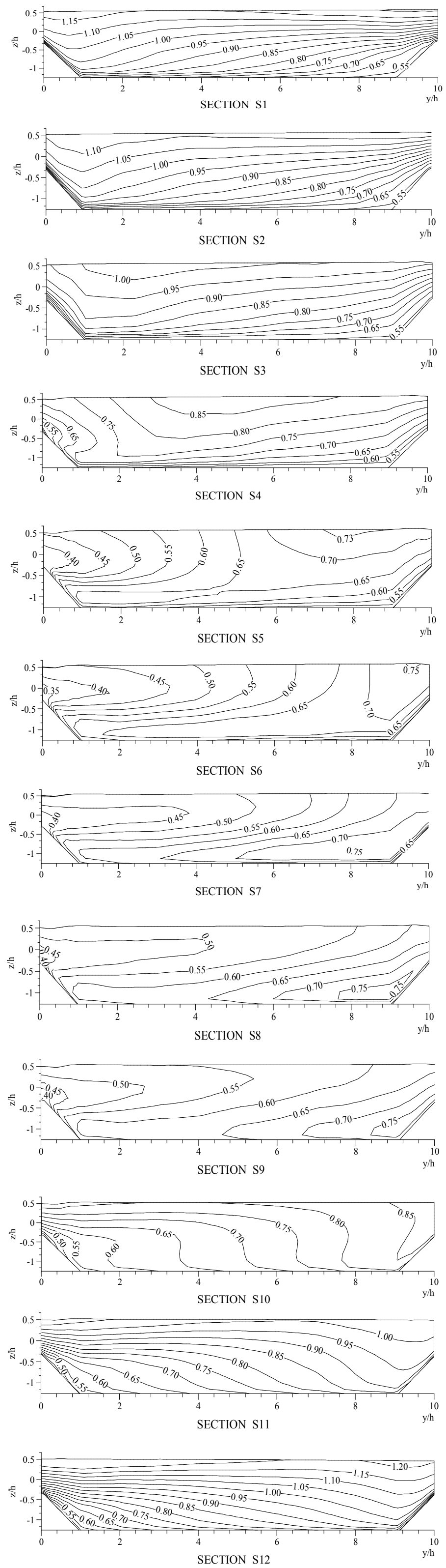

Figure 8

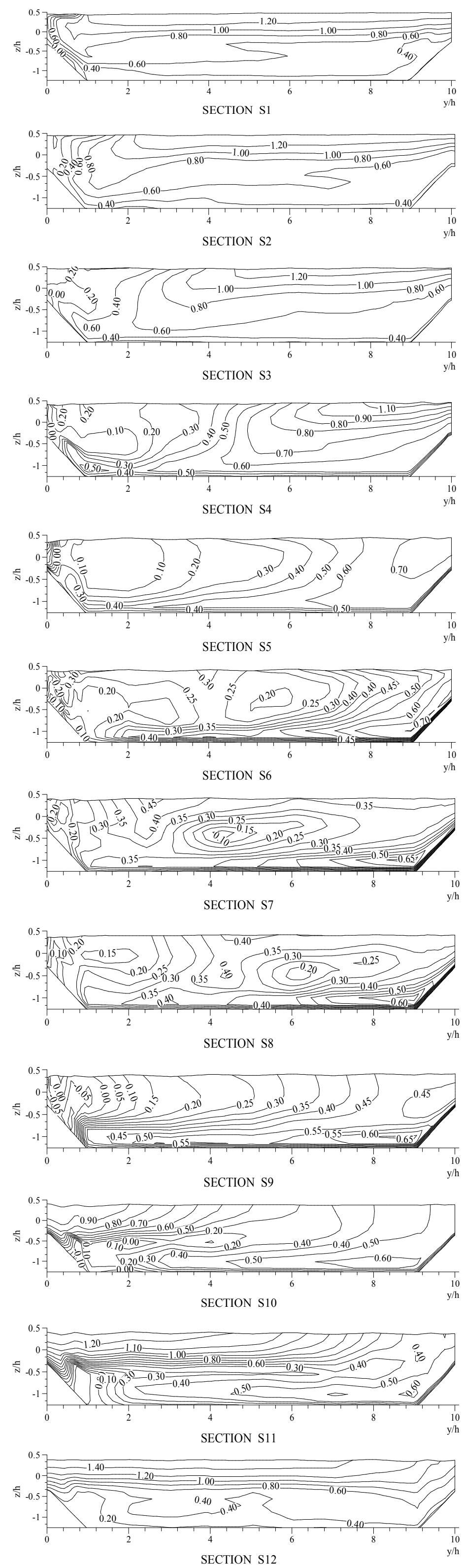

Figure 9

where higher positive lateral velocities are observed at most parts of the main channel and negative lateral velocities are observed near the bed. As the flow moves downstream to sections S10 to S12, the negative magnitudes of the lateral velocity in the main channel are seen, meaning that the flow is moving from the outer side towards the inner side of the main channel within the range -0.15U_s to -0.2U_s.

4.4 Secondary Flow Vectors

The results show the secondary vectors at sections S1 to S12 for non-vegetated floodplain as seen in **Figure 12**. At section S1, which is the apex section, a single dominant anticlockwise circulation cell, which occupies almost the whole main channel area, can be seen. As the flow moves downstream to section S3, the anticlockwise cell seen at section S1 disappears completely. However, the new clockwise circulation cell is seen near the inner side (left side) of the main channel. Thus it is evident that this new circulation cell originates from somewhere between section S1 and section S3. The generation of this new circulation cell at section S3 coincides well with the shearing of the main channel flow by the floodplain flow plunging into the main channel as clearly seen from the streamwise velocity and the lateral velocity profile at the same section**.** At section S5 which is the start of the cross-over region, the magnitude of the floodplain flow entering the main channel increases due to which the circulation cell seen at section S3, gains strength and size and travels towards the outer side of the main channel. This cell occupies most of the main channel inbank area at section S7, which is at the mid point of the cross-over region. The pattern of circulation remains almost the same at section S9 as it was at section S7. This suggests that the same magnitude of the floodplain flow entering the main channel maintains the same secondary flow along the cross-over region. At section S11, the magnitude of the secondary vectors at the bankful level near the inner side of the main channel is being reduced as expected. The secondary flow circulation pattern at section S12 is similar to that in section S1 except with the opposite sense of rotation.

However, **Figure 13** shows the secondary vectors for cross-over vegetated floodplain for sections S1 to S12. There are multiple secondary cells. As the flow moves downstream to section S2, a small clockwise cell is observed at the inner side of the main channel and a large single clockwise cell can be seen near the bed. The single clockwise circulation at the inner side of the main channel then moves towards the channel centreline until section S6. At the mid point of the cross-over sections S7 to S9, the complicated secondary circulations appear below the bankful level. Although there was no clear pattern of secondary flow cell on the right hand side, the strong lateral velocity moves towards the outer bank direction, and, as a result, pushes the maximum velocity closer to the outer side of the main channel. For sections S10 to S12, there are still a number of small-scale vortices appearing in the main channel although there are no blocks along the floodplain apex section. The secondary flow pattern shows a quite distinct difference, both at the apex region and at the cross-over section. Firstly, as seen at the apex region, at section S1 the secondary flow patterns are not stable with multiple circulation cells being seen for both cases. This is due the large eddy effect generated by the blocks placed along the cross-over section. Secondly in the cross-over region (sections S6 to S9), it can be seen that the circulation cells at the inner side of the main channel (left side) are quite different and strength compared to case non-vegetated floodplain. This is due to the fact that the blocks along the cross-over section cause a reduction in the magnitude of the floodplain flow entering the main channel. The vortices and wakes effect caused by the blocks are also noticeable for good portions of the main channel below the bankful level, which suggests that the flow in the main channel is not streamwisely dominant compared to case non-vegetated floodplain.

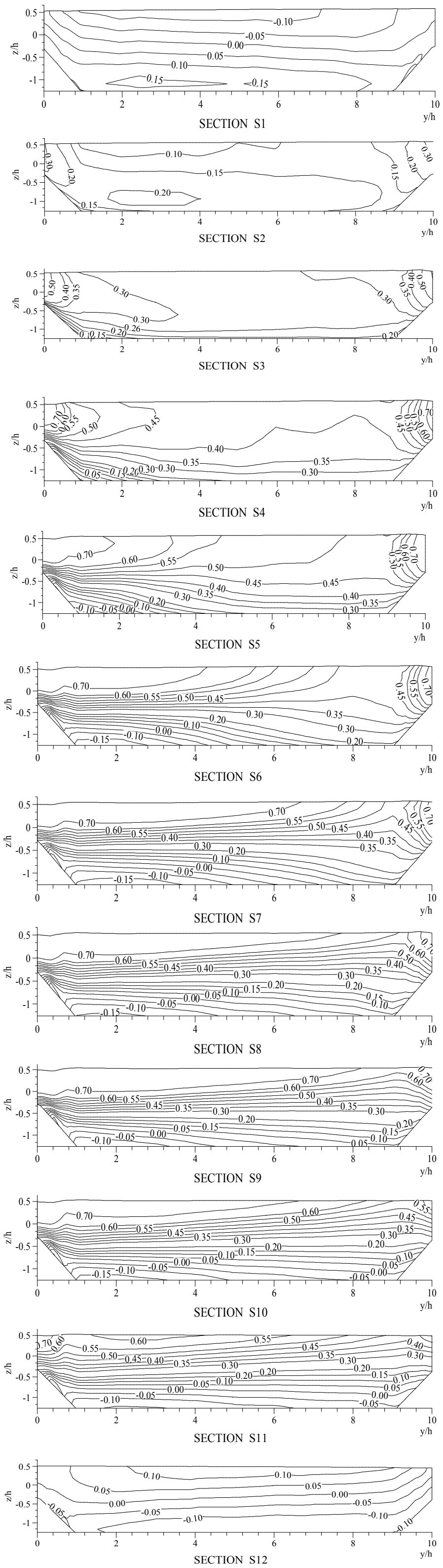

Figure 10

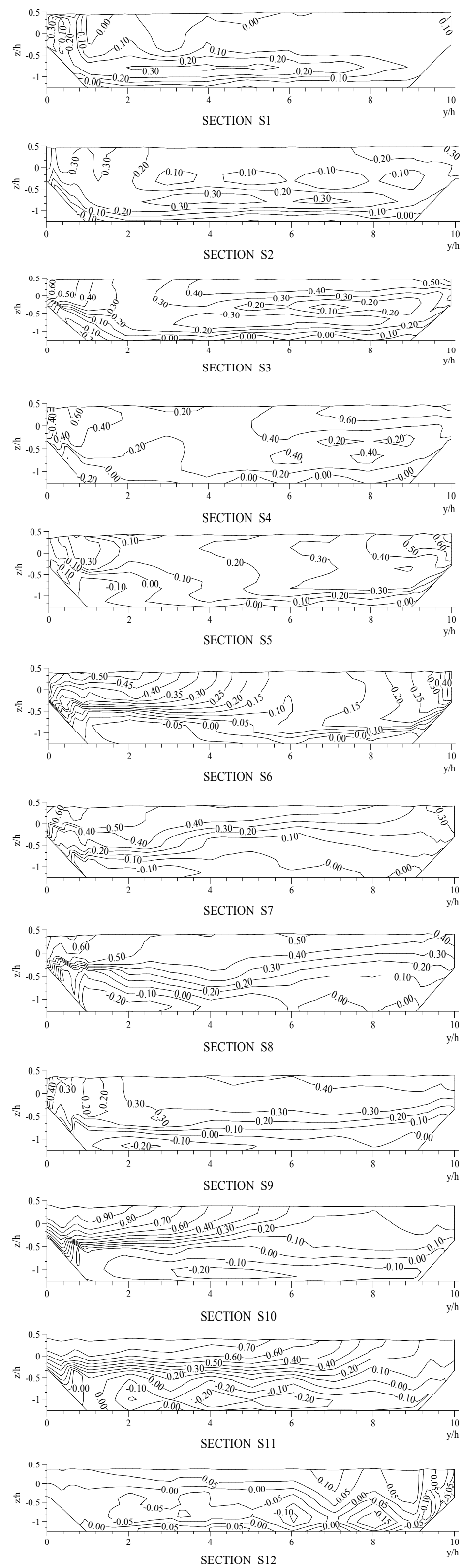

Figure 11

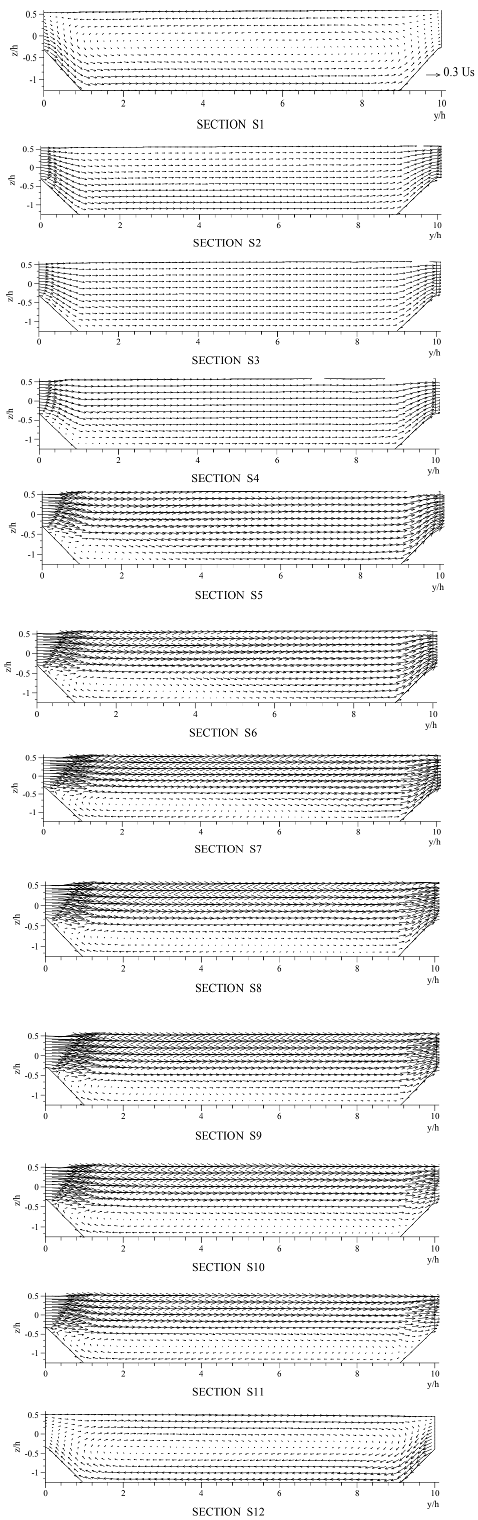

Figure 12

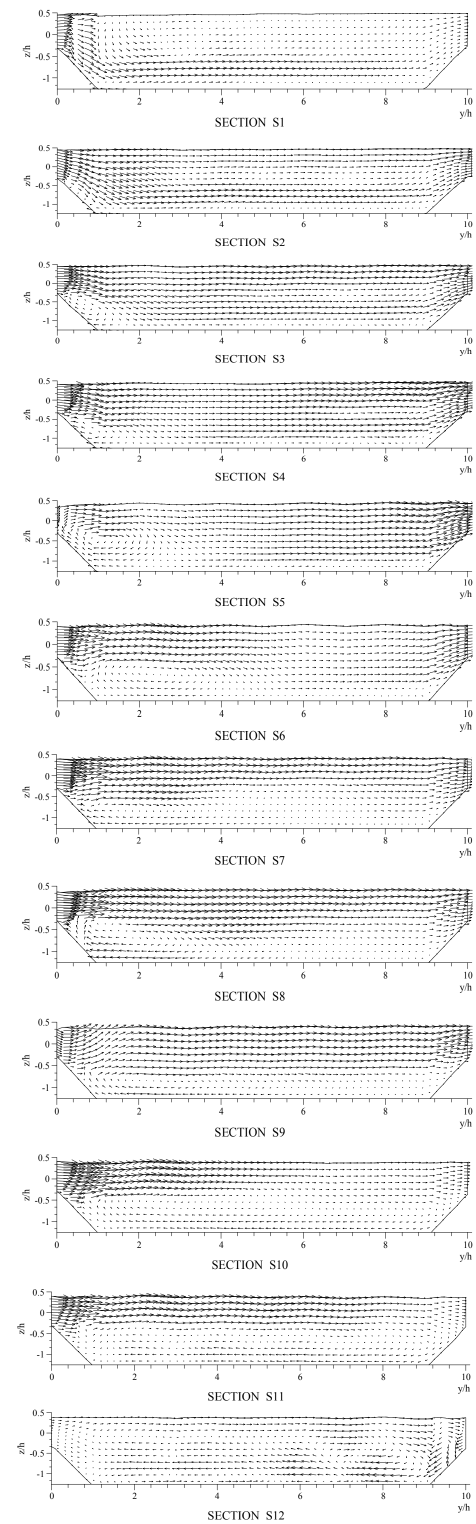

Figure 13

5. CONCLUSIONS

The depth-averaged velocity vector field for the non-vegetated floodplain case shows that the main channel flow generally follows the direction of the meander channel. The maximum velocity filament in the main channel stays close to the inner bank sidewall at the upstream apex and moves progressively to the outer bank as it approaches the downstream apex. However, for cross-over vegetated floodplain, along the cross-over section, the higher vortices occur near to the inner bank of the main channel behind the blocks and at the end of the cross-over section there are strong vortices produced by the blocks. The patterns of diverging and converging velocity vectors caused due to a series of blocks in the vegetated floodplain case. This indicates that large vortex interactions and wakes occurred within the main channel behind the blocks, which are strongly associated with the nature of the flow structures in a meandering channel for the vegetated floodplain case.

The most interesting feature of the compound meandering channel flow is the behaviour of the secondary flow. The secondary flow patterns are different for the non-vegetated floodplain and the cross-over vegetated floodplain. For the non-vegetated floodplain, the number of secondary flow cells in the main channel is attributed to the flow depth on the floodplain and the location of the section. In the cross-over vegetated floodplain case, there are multiple secondary flow cells across the apex section. The cross-over vegetated floodplain with continuous blocks along the cross-over section, particularly the vortices and wake extending directly across the cross-over section, are a feature of the secondary flows that have not been shown before. In general, cross-over vegetated floodplain with a roughened floodplain showed that the secondary flow cell is more vigorous in structure compared to non-vegetated floodplain. This subsequently leads to a larger energy loss.

REFERENCES

Hervouet, J. -M. (2000). "TELEMAC Modelling System: an Overview." *Hydrological Processes,* Vol. 14, pp. 2209-2210.

Ishigaki, T., Shiono, K. and Rameshwaran, P. (2002), PIV and LDA Measurements of Secondary Flow in a Meandering Channel for Overbank Flow, *Journal of Visualization*, Vol.5, No.2, pp.153-159.

Rameshwaran, P., Spooner, J., Shiono, K., and Chandler, J.H. (1999), Flow Mechanism in Two-Stage Meandering Channel with Mobile Bed, *Instn. Assoc. for Hydr Res. XXVIII* Biennial Congress, Graz, Austria, D6, pp 259.

Rameshwaran, P., & Naden, P. S. (2003). "3D Numerical Simulation of Compound Channel Flows." *Journal of Hydraulic Engineering,* Vol. 129, pp. 645-652.

Rameshwaran, P., & Shiono, K. (2002). "Predictions of Velocity and Boundary Shear Stress in Compound Meandering Channel." *River Flow 2002, International Conference on Fluvial Hydraulics*, Vol. 1, pp. 223-231.

Shiono, K. and Muto, Y. (1998), Complex flow mechanisms in compound meandering channel for overbank flow*, Journal of Fluid Mechanics*, Vol. 376, pp. 221-261.

Shiono, K., Spooner, J., Rameshwaran, P., & Chandler, J. (2001), Energy Losses in Meandering Channels with Flat Bed and Natural Beds For Overbank Flows, *Proc. of the XXIX IAHR Congress,* Vol. 1, pp. 256-263.

TECHNICAL CONTRIBUTIONS

Turbidity Currents